

RESEARCH

Open Access



Imaging features and consideration of progression pattern of diffuse hemispheric gliomas, H3 G34-mutant

Yuji Kibe^{1,2†}, Lushun Chalise^{1,3†}, Fumiharu Ohka^{1*}, Kazuya Motomura^{1,2}, Norimoto Nakahara³, Kosuke Aoki¹, Shoichi Deguchi¹, Yoshiki Shiba¹, Kazuhito Takeuchi¹, Kenichiro Iwami¹, Junya Yamaguchi¹, Hiroki Shimizu¹, Sachi Maeda¹, Yuhei Takido¹, Ryo Yamamoto¹, Yusuke Okuno⁴, Akihiro Sakai⁵, Kennosuke Karube⁶ and Ryuta Saito¹

Abstract

Diffuse hemispheric glioma H3 G34-mutant (DHG) has been identified as a distinct pediatric-type high-grade glioma, according to the World Health Organization (WHO) classification of central nervous system tumors. Widely accepted treatment options include surgery, radiation, and conventional chemotherapy. However, the efficacy of the surgical resection remains unclear. Although there are some reports, a comprehensive understanding of the clinical characteristics, pathogenesis, and outcomes of DHG is insufficient to evaluate the efficacy of maximal tumor resection. We retrospectively analyzed nine cases of DHG, focusing on imaging features and progression patterns. Initial Magnetic Resonance Imaging (MRI) revealed T2/FLAIR high lesions with minimal or no contrast enhancement in all cases. The lesions exhibited T2/FLAIR hyperintensities and focal diffusion restriction in the deep white matter, with most showing high methionine accumulation, suggesting deep white matter infiltration at the time of diagnosis. The extent of white matter infiltration in tumor resection cases was significantly negatively correlated with the extent of resection (EOR). In addition, cases with EOR of 90% or more had significantly longer progression-free survival (PFS) and overall survival (OS). However, achieving an EOR of 90% or more was possible in fewer than half of the cases, primarily in those with relatively limited white matter involvement. Histopathological findings of the tumor obtained by initial resection and autopsy revealed extensive deep white matter infiltration, with one patient demonstrating tumor invasion into the brainstem at death. Our study highlights early deep white matter infiltration of DHGs, complicating surgical resection, and potentially contributing to a poor prognosis. While EOR may influence survival to some extent, residual lesions extensively infiltrate the white matter and eventually invade the brainstem and contralateral brain, thereby contributing to mortality. These findings underscore the challenges of managing DHGs and emphasize the need for further research on effective therapeutic strategies, particularly to understand and target their unique progression patterns.

Keywords Diffuse hemispheric glioma, G34-mutant, Deep white matter infiltration, Surgical resection

[†]Yuji Kibe and Lushun Chalise contributed equally to this work.

*Correspondence:

Fumiharu Ohka

ooka.fumiharu.j7@f.mail.nagoya-u.ac.jp

Full list of author information is available at the end of the article



Introduction

Diffuse hemispheric glioma, H3 G34-mutant (DHG), emerges as a distinct pediatric-type diffuse high-grade glioma in the fifth edition of the World Health Organization (WHO) Classification of Tumours of the Central Nervous System [20]. This aggressive brain tumor, with characteristics distinct from those of other established types of adult central nervous system (CNS) WHO grade 4 gliomas, primarily manifests in the cerebral hemisphere of adolescents and young adults. They are most frequently located in the cerebral hemispheres, especially in the frontoparietal lobes, with occasional spreading to midline structures and leptomeningeal dissemination [15, 21]. DHGs are characterized by mutations in the histone gene H3F3A (H3.3), resulting in the substitution of glycine at position 34 with arginine or valine (G34R/V) [28, 37, 46, 49]. These non-midline hemispheric high-grade gliomas are exclusive to IDH mutations and mutually exclusive to H3 K27M mutations associated with midline gliomas. DHGs are rare tumors, comprising less than 1% of all gliomas and occurring at roughly half the frequency of H3 K27M mutations. However, they account for 15% of high-grade gliomas in adolescents and young adults, disproportionately affecting younger populations [28, 37, 49]. The median age at diagnosis in DHGs is around 18–19 years, and patients with DHGs exhibit a relatively more favorable prognosis compared to both “Glioblastoma, IDH-wildtype” and “Diffuse midline glioma, H3 K27-altered” [10, 14, 42]. Nevertheless, they inevitably experience disease recurrence and mortality under the current treatment regimens; hence, exploring potential therapeutic strategies is critical.

Surgical tumor removal, followed by radiation and chemotherapy, remains the standard treatment strategy for malignant gliomas. However, the effectiveness of maximal surgical resection for DHGs remains unclear, underscoring the critical need for a deeper insight into these aspects to develop better therapeutic strategies. While glioma patients generally survive longer in cases with a greater extent of tumor resection, the role of surgical treatment in DHGs and whether the extent of resection has any prognostic implications for this novel glioma subtype remain uncertain [3, 39]. Surgical resectability and postsurgical tumor progression may depend on the radiological features and localization of gliomas in the brain because gliomas usually arise from the edges of the surgical cavity [2, 31, 32, 38]. Therefore, this article presents a comprehensive examination of the radiological features of DHG to reveal key tumor characteristics and progression. Despite some existing reports on this novel tumor type, a comprehensive understanding of the clinical characteristics, pathogenesis, and outcomes of DHGs is yet to be achieved [33, 45]. In this study, we

retrospectively analyzed nine cases of DHGs, with a specific focus on imaging features and progression patterns, to contribute to our understanding of this unique glioma subtype.

Materials and methods

Patient data

Nine patients treated between March 2015 and June 2021 at Nagoya University Hospital (Nagoya, Japan) were diagnosed with DHGs. All patients underwent surgery, tumor resection, or biopsy under general anesthesia at the Nagoya University Hospital or Nagoya Central Hospital (an affiliated hospital of the Nagoya University Department of Neurosurgery). Maximal safe tumor resection, with routine use of neuronavigation, neuromonitoring, and intraoperative Magnetic Resonance Imaging (MRI), was attempted whenever the tumor formed a singular mass, leading to a significant mass effect. If the intraoperative MR image showed any tumor that could be safely resected, the remaining tumor was resected as much as possible up to the functional boundary, as previously described [24]. An integrated diagnosis of DHG was made for all tumors by combining histopathological features and H3 G34R/V detection using Sanger sequencing. Patient clinical information and outcomes, including age, sex, histopathological findings, extent of resection, prescribed adjuvant therapy, radiographic findings before and after treatment, progression-free survival (PFS), and overall survival (OS), were retrospectively analyzed.

Extent of resection (EOR) was defined as the resection of a T2/FLAIR high-intensity lesion. While the EOR of other grade 4 gliomas is usually defined as the resection of gadolinium (Gd)-enhanced lesions on Magnetic Resonance Imaging (MRI), T2/FLAIR high-intensity lesions were used to calculate the extent of resection because DHGs were not necessarily Gd-enhanced. We measured the EOR using volumetric analysis with iPlan Cranial 3.0.6 software (Brainlab AG). The EOR was calculated as the percentage of (Preoperative Tumor Volume-Postoperative Tumor Volume)/Preoperative Tumor Volume. Abnormal T2/FLAIR lesions were used for volumetric analysis.

PFS and OS were defined as the duration from initial surgery to recurrence and death, respectively. One patient underwent an autopsy examination after death.

MR and PET imaging

MR was performed using GE 3.0T scanners (GE Genesis Signa and Signa HD; GE Healthcare, Milwaukee, WI, USA) and Siemens 3.0T scanners (TrioTim and Verio; Siemens Healthcare GmbH, Erlangen, Germany). The MRI protocol included pre- and post-contrast T1-weighted, T2-weighted, and FLAIR imaging.

Contrast-enhanced T1-weighted images were acquired after administration of 0.1 mmol/kg gadopentetate dimeglumine.

Positron emission tomography (PET) images were acquired using a Headtome-V PET camera (Shimadzu, Kyoto, Japan) with a spatial resolution of 4.5 mm (axial) and a full width at half maximum of 3.9 mm (transaxial) at the center of the field of view. The PET tracers were intravenously injected at a dose of 11.1 MBq/Kg for 11C-methionine (MET) PET scan and 3.7 MBq/Kg for 18F-fluorodeoxyglucose (FDG) PET. All emission scans were performed in 2D acquisition mode, and the reconstructed images were attenuated using filtered back projection [30].

Imaging analysis

Among radiological findings, we evaluated the following parameters:

- Tumor location, Margin (ill-defined, well-delineated)
- Enhancement pattern on gadolinium-enhanced MRI (none, faint, partial)
- Diffusion restriction: (ADC values of the tumors were measured, and diffusion restriction was defined as a mean ADC value lower than $1.25 \times 10^{-3} \text{ mm}^2/\text{s}$) [5].
- Uptake of 11C-methionine in PET
- Uptake of 18F-fluorodeoxyglucose (FDG) in PET
- Initial white matter lesions (cerebral peduncle, internal capsule, corona radiata, temporal stem, anterior commissure, and corpus callosum)
- Terminal stage white matter lesions (cerebral peduncle, internal capsule, corona radiata, temporal stem, anterior commissure, and corpus callosum)

Deep white matter lesions evaluation

In this study, we evaluated and scored six locations (the Cerebral Peduncle, Internal Capsule, Corona Radiata, Temporal Stem, Anterior Commissure, and Corpus callosum) of deep white matter lesions. These locations were chosen because they involve representative projections, associations, and commissural fibers of cerebral white matter [4, 40]. Each location was assigned a score of one. In cases where lesions spanned multiple brain lobes or extended from the brain surface to broader regions, such as the basal ganglia, we considered white matter structures along the connecting line as part of the infiltration area. We calculated the White Matter Lesion (WML) score for each case, assigning one point to the presence of each white matter lesion.

DNA extraction from tumor and blood samples

Intraoperative tumor samples were collected. DNA was extracted from frozen tumors and blood samples using the QIAamp DNA Mini Kit (Qiagen, Hilden, Germany) according to the manufacturer's instructions. The amount of DNA obtained was evaluated using the Qubit dsDNA HS Assay Kit (Invitrogen, Paisley, Scotland). DNA was extracted from formalin-fixed paraffin-embedded (FFPE) tumor samples using the GeneRead DNA FFPE Kit (Qiagen) according to the manufacturer's instructions.

Sanger sequencing

Sanger sequencing was performed to detect H3F3A mutations in the DNA extracted from the tumor samples. We amplified a 194-base pair (bp) fragment for DNA spanning the sequence encoding histone H3 glycine (G) 34 of the H3F3A gene. We applied a conventional PCR involving the following steps: 35 cycles with denaturation at 98 °C for 10 s, annealing at 55 °C for 30 s, and extension at 68 °C for 30 s, with a final extension step at 68 °C for 5 min; the forward primer (5'-TGCTGGTAGGTAAGT AAGGAG-3') and reverse primer (5'-AGCAGTAGT TAAGTGTTC AAATG-3') were used. Sequence analysis was performed using ApE v2.0.55.

Whole-genome sequencing (WGS)

DNA libraries were prepared using the TruSeq DNA PCR-Free Library Prep Kit (Illumina, San Diego, CA, USA) according to the manufacturer's instructions. The NovaSeq6000 platform (Illumina) was used to sequence and generate 400-bp long paired-end reads. A median of 676,766,942 reads per sample were obtained and aligned to cover the hg19 reference genome with 31.6× coverage using the Burrows–Wheeler aligner (<http://bio-bwa.sourceforge.net/>) with default parameters and a -mem option. Sequence variations were detected and annotated using VarScan2 (<http://dkoboldt.github.io/varscan/>). For copy number analysis, the coverage of each 10kb span was compared with the mean coverage of the entire genome. The data were segmented by circular binary segmentation using DNACopy 1.56.0 with modified parameters.

FoundationOne CDx testing

FoundationOne CDx is a CGP platform that applies NGS to in vitro diagnostics using a hybrid capture-based target enrichment approach and whole-genome shotgun library construction to identify all four classes of somatic genomic alterations including substitutions, insertions, deletions (indels), copy number alterations, and select rearrangements. The typical median depth of coverage is > 500×. The FoundationOne CDx Panel detected

alterations in 324 genes. These genes included all coding exons of 309 cancer-related genes, one promoter region, one non-coding RNA, and selected intronic regions of 34 commonly rearranged genes; 21 coding exons were also included. Tumor mutation burden (TMB) and microsatellite instability (MSI) status were analyzed simultaneously (detailed information is available at <https://www.foundationmedicine.com/genomic-testing/foundation-one-cdx>) [43].

Results

Patient characteristics

Nine patients were diagnosed with diffuse hemispheric glioma at the Department of Pathology, Nagoya University Hospital. H3 G34R was detected by Sanger sequencing in all tumors. Patient characteristics and treatment histories are summarized in Table 1. The mean age at onset was 20.2 years (range 10–26 years).

Five patients (55.6%) were female and four (44.4%) were male. All tumors were supratentorial, with two tumors in the frontal lobe, two tumors in the parietal lobe, one tumor each in the insula and temporal lobe, and three tumors extending to two or more brain lobes (Table 2). Surgical resection with craniotomy was performed in eight patients (88.9%), whereas tumor biopsy was performed in one patient. Initial histopathological diagnosis classified four tumors as glioblastoma (GBM), four tumors as central nervous system embryonal tumors (CET), and one as anaplastic astrocytoma (AA). WGS and FoundationOne CDx revealed mutations of *H3F3A* (H3 G34R), *TP53* and *ATRX* in all analyzed cases (cases 1, 2, 3, 5 and 6). Additionally, *EGFR* amplification was observed in case 1, and *PDGFRA* mutations were identified in three cases (cases 3, 5, and 6) (Supplementary Fig. 1). All patients were treated with chemotherapy and radiotherapy after diagnosis (Table 1).

Table 1 Clinical characteristics of patients of DHGs-G34m

Case	Sex	Age	Histology	H3F3A	Treatment			Outcome	
					EOR	CT	RT	PFS (m)	OS (m)
1	Female	12	CET→GBM	G34R	94%	TMZ, BEV	60Gy	2.1	26.2
2	Female	22	CET	G34R	95%	CARE, TMZ, ETP, BEV	CSI25.2Gy boost36Gy	33.1	48.3
3	Female	20	GBM	G34R	74%	TMZ, BEV, TTF	60Gy	3.0	13.4
4	Female	11	GBM	G34R	98%	TMZ	60Gy	71.4	87.4
5	Male	14	GBM	G34R	73%	TMZ, BEV	60Gy	1.6	8.9
6	Male	10	CET	G34R	100%	TMZ	60Gy	15.6	27.4
7	Male	26	AA	G34R	Biopsy	TMZ, BEV	60Gy	3.2	17.2
8	Male	17	GBM	G34R	58%	TMZ	60Gy	1.3	Alive
9	Female	50	CET	G34R	73%	TMZ	60Gy	1.4	Alive
Mean		20.2						14.7	32.7

EOR, Extent of resection; CT, Chemotherapy; RT, Radiation therapy; PFS (m), Progression free survival (month); OS (m), Overall survival (month); CET, Central nervous system embryonal tumor; GBM, Glioblastoma; TMZ, Temozolomide; BEV, Bevacizumab; CARE, Carboplatin and etoposide; ETP, Etoposide; CSI, Craniospinal irradiation; TTF, Tumor-treating field; AA, Anaplastic astrocytoma

Table 2 Initial radiographic features of DHGs-G34m

Case	Location	Margin	Contrast enhancement	Diffusion restriction	MET-PET	FDG-PET
1	Frontal	Well	Faint	Yes	Very high	Partial
2	Frontal	Well	Partial	Yes	Very high	Low
3	Parietal	Ill	Faint	Yes	Very high	Low
4	Parietal	Well	Partial	Yes	n/a	n/a
5	Insula	Ill	None	Yes	Very high	Partial
6	Temporal	Ill	None	Yes	n/a	n/a
7	Multiple	Ill	None	Yes	High	Low
8	Temporal, parietal	Ill	Faint	Yes	High	n/a
9	Temporal, occipital	Ill	Faint	Yes	n/a	n/a

MET-PET, [11C] methionine positron emission tomography; FDG-PET, [18F] fluorodeoxyglucose positron emission tomography; n/a, No data available

Radiographic characteristics

Initial MRI revealed T2/FLAIR high lesions with poor contrast enhancement in all cases (Fig. 1). Three of the nine tumors (33.3%) showed no contrast enhancement (Table 2). Three (33.3%) tumors with faint-to-partial contrast enhancement exhibited well-defined margins at initial presentation. All tumors (100%) demonstrated restricted diffusion on MRI. Six patients (66.7%) underwent preoperative positron emission tomography (PET). High accumulation of methionine (MET) and low or partial accumulation of FDG were observed in

all cases (Table 2 and Fig. 1A). The MET-accumulated area corresponded to T2/FLAIR high lesions, suggesting that all T2/FLAIR high lesions were tumor components rather than edema. The MET-accumulated area also corresponded to areas of diffusion restriction, confirmed as non-intratumoral bleeding through preoperative SWI or T2* images (Fig. 1B). All tumors also harbored T2/FLAIR high lesions in the deep white matter, including the internal capsule, corona radiata, temporal stem, and corpus callosum (Table 3). Most of these lesions showed high MET accumulation,

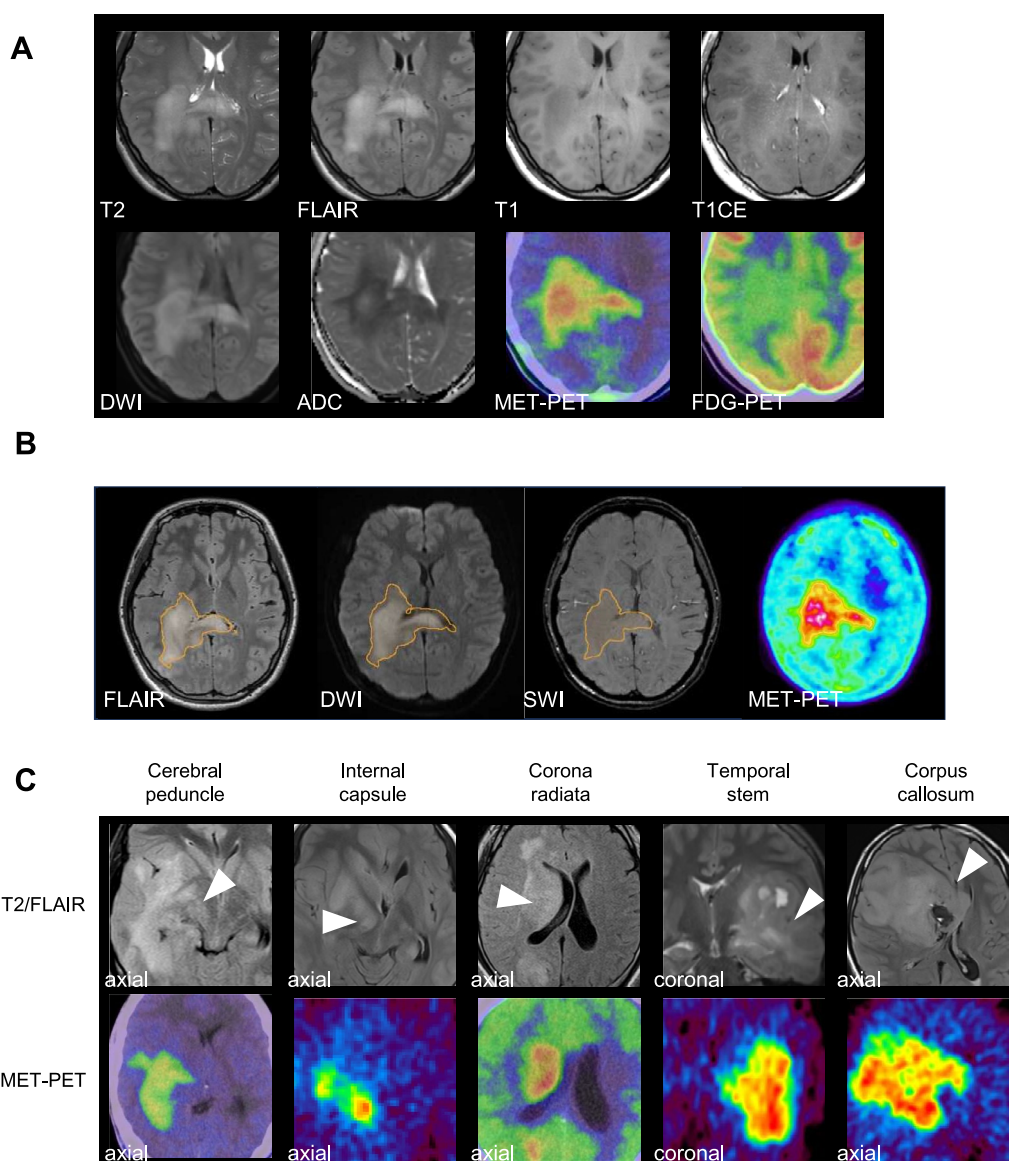


Fig. 1 Initial radiographical features and white matter lesions. **A** MRI, Methionine (MET) PET and FDG-PET images of case 3. **B** MRI and MET-PET images of case 3. Orange line reveals methionine high uptake region. **C** Deep white matter lesions at initial presentation. The upper row shows T2/FLAIR images, and the lower row shows MET-PET images of the corresponding cases. From left side, case 8, case 1, case 7, case 5, case 1

Table 3 Initial white matter lesion and EOR

Case	Cerebral peduncle	Internal capsule	Corona radiata	Temporal stem	Anterior commissure	Corpus callosum	EOR
1	Yes	Yes	Yes	No	No	Genu	94%
2	No	No	No	Yes	No	No	95%
3	No	Yes	Yes	Yes	No	Splenium	74%
4	No	No	Yes	No	No	No	98%
5	Yes	Yes	No	Yes	Yes	No	73%
6	No	No	No	Yes	No	No	100%
7	Yes	Yes	No	Yes	Yes	No	Biopsy
8	Yes	Yes	Yes	Yes	No	Splenium	58%
9	Yes	Yes	Yes	Yes	No	Splenium	73%

EOR, Extent of resection

suggesting that the DHGs had deep white matter infiltration at the initial diagnosis (Fig. 1C).

Treatment and outcome

Tumors in eight of nine patients (88.9%) were surgically resected. An extent of resection (EOR) of 90% or more was achieved in four (44.4%) cases (Table 1). A biopsy was performed in one case.

The white matter lesion (WML) score in cases with tumor resection showed a significantly negative correlation with EOR ($R^2=0.688$, $p=0.01$) (Fig. 2A). Median progression free survival (PFS) in cases with an EOR of 90% or more was significantly longer than in cases where EOR was less than 90% (24.4 months vs 1.6 months, $p=0.032$) (Fig. 2B). Overall survival in cases with an EOR of 90% or more was also significantly longer than in cases with EOR of less than 90% (37.3 months vs 13.4 months, $p=0.01$) (Fig. 2C).

Tumor progression in DHGs

The clinical course of case 3 is shown as a representative case (Fig. 3A–D). Tumor resection was performed for residual lesions in the corona radiata and corpus callosum. After partial resection, concurrent treatment with radiation therapy (60 Gy/30 Fr) and temozolomide (TMZ) (Stupp regimen) was administered. However, 3 months later, the residual lesions progressed rapidly along the deep white matter. Although combination therapy with TMZ, bevacizumab (BEV), and tumor-treating field (TTF) achieved a partial response, the lesions eventually expanded to the bilateral temporal lobes and brainstem. The patient died 13 months after surgery. MRI at the terminal stage of each case showed tumor infiltration into the cerebral peduncle via the pyramidal tract and into the contralateral brain via the corpus callosum or anterior commissure in six and seven cases, respectively (Supplementary Table 1).

Autopsy findings

An autopsy performed in one patient (case 3) revealed atypical glial cells with a high N/C ratio that densely proliferated around the surgical cavity, consistent with the histopathological findings of the initial tumor. Extensive infiltration of the tumor cells into the bilateral temporal lobes and brainstem was observed. In addition, tumor cells were observed in the internal capsule passing through the lenticular nucleus, demonstrating infiltration of DHGs along the deep white matter (Fig. 3E, Supplementary Fig. 2).

Discussion

DHGs are pediatric-type brain tumors that have emerged as unique entities according to the latest WHO classification [20]. Because this is a rare tumor, especially in adults, little is known about its pathophysiology or natural history [47].

The mean age of the patients at diagnosis in our series was 20.2 years. Although DHGs are usually regarded as pediatric gliomas, they affect young adults, and our data agree with similar age groups previously reported [28, 37, 45, 49]. The mean overall survival in our case series was 32.7 months. Notably, one female patient who underwent gross total resection survived for more than 7 years, exceeding the longest survival previously reported [47]. All tumors in our series had a glycine-to-arginine (G34R) mutation, which may have contributed to the slightly better survival observed, compared with the glycine-to-valine (G34V) mutation [45]. WGS and FoundationOne CDx revealed molecular alterations (Supplementary Fig. 1), including mutations of *TP53* and *ATRX*, consistent with prior studies [7, 15, 33, 45]. Among the 9 cases in this study, 4 tumors were initially diagnosed as CET, with the initial histopathology showing small round cell tumors with high N/C ratio. These cases can be

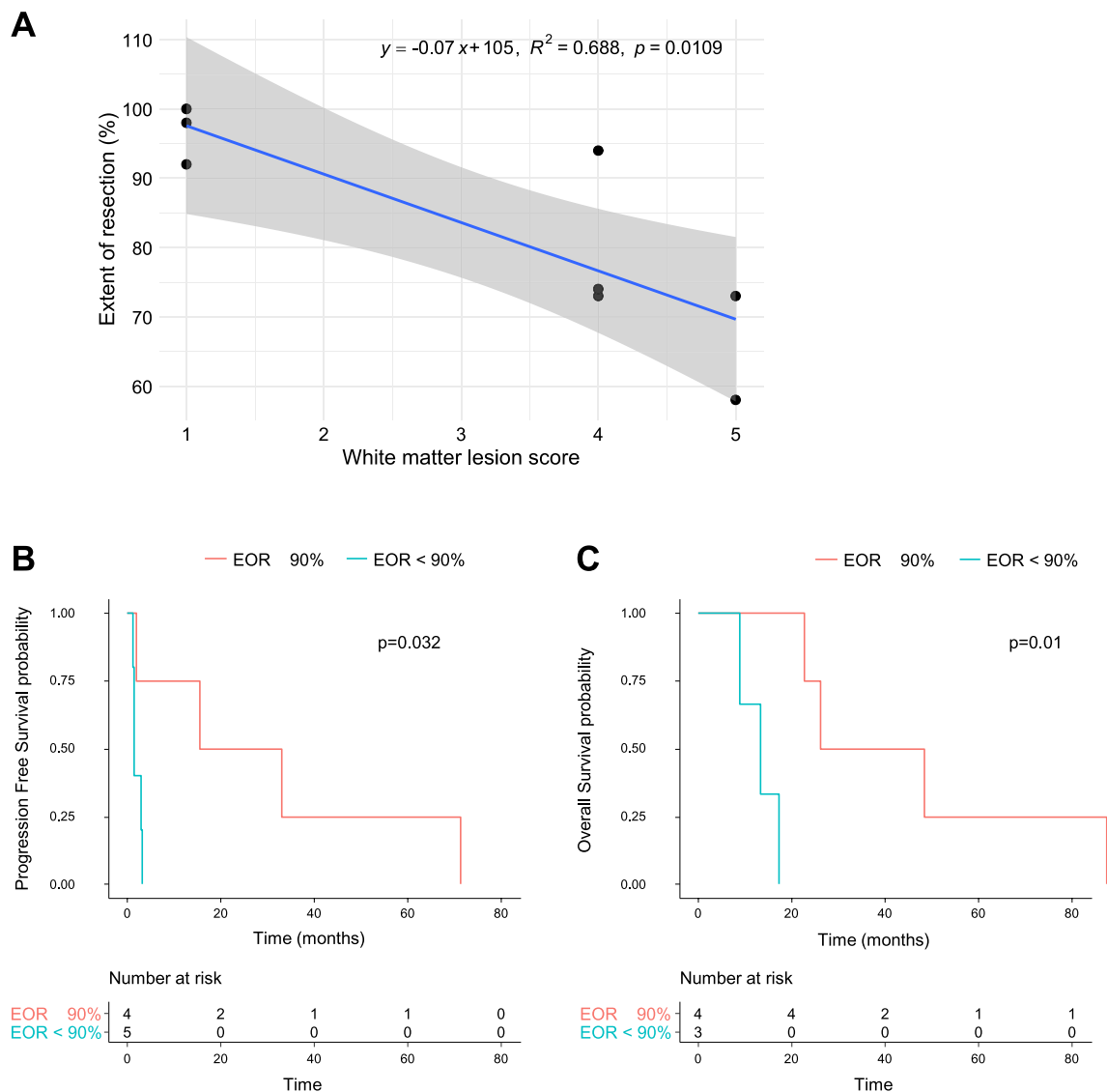


Fig. 2 **A** Scatter plot and linear correlation analysis depicting the relationship between white matter lesion score and extent of resection (EOR), calculated using Pearson correlation coefficient, in cases where tumors were surgically resected via craniotomy. The blue line represents the linear regression model, whereas the gray zone represents the 95% confidence interval. **B** Kaplan–Meier survival curve demonstrating Progression Free Survival (PFS) of the two groups (Extent of resection, EOR of 90% or more vs EOR of less than 90%). **C** Kaplan–Meier survival curve demonstrating Overall Survival (OS) of these two groups

categorized as DHG H3G34 mutants with embryonal features, as previously reported [6, 7, 12, 23].

MRI performed at diagnosis showed T2/FLAIR high lesions with poor contrast enhancement and restricted diffusion in all cases. High methionine accumulation and moderate FDG accumulation were observed in all cases, with the MET-accumulated area corresponding to the T2/FLAIR high lesion. This finding suggests that all T2/FLAIR high lesions in the deep white matter represented the tumor itself rather than edema. Another striking feature in this series was focal diffusion

restriction, characterized by high-intensity areas on diffusion-weighted images, possibly indicating the presence of an aggressive hypercellular tumor with a poor prognosis [34, 35, 44]. While MET-PET may offer superior diagnostic capabilities for assessing tumor extension and tumor cell density in gliomas [18, 27, 29], the consistency of the MRI and MET-PET findings in our series suggests that MRI alone can adequately evaluate tumor expansion when PET is unavailable. Moreover, preoperative SWI or T2* sequences confirmed the areas of diffusion restriction as non-intratumoral

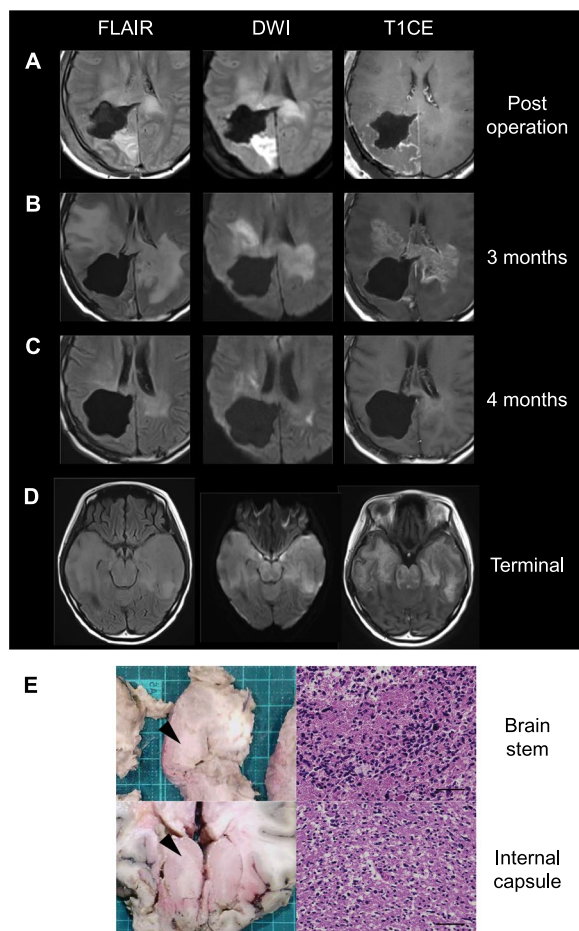


Fig. 3 Clinical course of case 3. **A** Post operative MRI, **B** MRI 3 months after tumor removal, **C** MRI 4 months after tumor removal and **D** MRI 13 months after tumor removal. Each image includes FLAIR (left), DWI (middle) and T1CE (right) images. **E** Extensive infiltration along deep white matter in histopathological findings. Macroscopic images of each site obtained by autopsy (left). Hematoxylin-eosin staining of the specimens from each site (right). Scale bar indicates 100 μ m

bleeding, suggesting that the diffusion restriction reflected a distinct characteristic of the tumor rather than hemorrhage.

The WML score showed a strong negative correlation with EOR in our case series, clearly indicating that white matter infiltration is a limiting factor for EOR in DHGs. Cases with an EOR of less than 90% had significantly worse prognosis, indicating that WML limits EOR and acts as a poor prognostic factor in these tumors. Although statistical significance was not observed for OS, possibly due to the limited number of cases in this study, a trend toward worse prognosis was noted in cases with high WML scores (Supplementary Fig. 3).

An EOR of 90% or more was achieved in less than 50% of the cases in this study. Although we routinely

employed a strategy of maximal safe resection utilizing navigation and intraoperative MRI in all possible glioma cases, the EOR in this series of DHGs was lower than that achieved in our previous glioma studies [25, 26]. This outcome is likely due to the early infiltration of DHGs into the deep white matter, which poses a formidable challenge for surgical resection. On the other hand, in cases with minimal initial white matter infiltration (cases 2, 4 and 6), a higher EOR was achieved, corresponding to better survival in our series, which is generally consistent with those in diffuse gliomas [3, 22, 25, 39, 41]. An EOR of 90% or more significantly increased both the PFS and OS in this study which is in concordance with the report by Crowell et al. that more than near-total resection is associated with a better prognosis in DHGs [7]. It has also been reported that the DHG cases with well-defined margins, implying low white matter infiltration, showed better survival rates [16]. Studies have shown that radical resection, including T2/FLAIR high-intensity areas, may improve the prognosis for malignant gliomas [13, 36]. Additionally, case reports from our group and others have shown prolonged survival after supratotal resection of the tumor beyond the radiologically marked tumor border [11, 48].

Extensive white matter infiltration often limits the EOR, and incomplete resection is generally associated with poor outcomes in glioma [9, 17, 19, 26]. However, this study is, to our knowledge, the first to demonstrate that a higher EOR may improve prognosis even in highly infiltrative tumors such as DHG. Although complete resection was rarely achievable, cases like Case 1 (WML score of 4) showed that safe resection of tumors with significant white matter infiltration is possible. In this case, an EOR of over 90% was achieved, which may have contributed to improved survival. While the precise impact of aggressive resection on survival remains uncertain, even modest prolongation of survival may hold significant value for the young patients with DHG. Therefore, we propose that aggressive surgical resection should be attempted in cases of DHG where it can be safely performed.

Despite the limited number of cases, our study showed that DHGs are infiltrative tumors that expand throughout the T2 high-intensity areas, thus making radical resection virtually impossible. The residual tumor eventually infiltrates the brainstem and contralateral brain, leading to patient death. Although current therapies have improved local tumor control, patients with malignant glioma still have a poor prognosis, with the majority succumbing to tumor infiltration into the brainstem or dissemination [1, 8]. Infiltration to the brainstem and contralateral brain

was pathologically confirmed in our autopsy case. To the best of our knowledge, this is the first study to report evidence of brainstem infiltration as the cause of death in DHG using multiple modalities, such as MET-PET and histopathological findings.

In our DHG cases, deep infiltration was found at initial diagnosis, indicating that DHG had a greater tendency to invade the white matter than glioblastoma. One of the main reasons for the poor prognosis of DHGs is that they present with deep white matter infiltration at initial onset, making radical resection difficult, especially along the midline, making them prone to further deep infiltration towards the brain stem. Considering the radiological features of DHGs, improving prognosis through surgical strategies alone may not be practical. Therefore, further research into the molecular characteristics of these tumors appears essential for enhancing patient outcomes.

Study limitations

The major limitations of our study were the limited sample size, retrospective design, and the absence of a comparative pediatric and other CNS WHO grade 4 glioma series. Statistical bias due to the limited number of cases suggests that these results need to be validated in a larger prospective study. Nevertheless, this study provides valuable information regarding the radiological features and possible tumor progression of DHGs.

Conclusions

DHGs exhibited deep white matter infiltration at the time of initial onset. Although surgical resection may influence the prognosis of these tumors to some extent, complete resection is nearly impossible. Residual lesions extensively infiltrate the white matter and eventually invade the brainstem and the contralateral brain, leading to patient death.

Abbreviations

DHG	Diffuse hemispheric glioma, G34-mutant
WHO	World Health Organization
EOR	Extent of resection
OS	Overall survival
PFS	Progression-free survival
MRI	Magnetic resonance imaging
PET	Positron emission tomography
MET	Methionine
FDG	Fluorodeoxyglucose
WML	White matter lesion
FFPE	Formalin-fixed paraffin-embedded
HE	Hematoxylin and eosin
IHC	Immunohistochemistry
WGS	Whole-genome sequencing
TMZ	Temozolomide
BEV	Bevacizumab
TTF	Tumor treating fields

Supplementary Information

The online version contains supplementary material available at <https://doi.org/10.1186/s40478-025-01945-w>.

Additional file 1: Figure S1. Gene mutations, copy number alterations, and chromosomal alterations in Case 1, 2, 3, 5 and 6. Gene mutations (green box), focal amplification (red square), gene gain (pink square), homozygous deletion (blue square) and heterozygous deletion (light blue square) of cyclins/Rb-related genes, mismatch repair genes, TP53-related genes, RTK/Ras/PI3K/AKT genes, chromatin modifiers, histone H3, IDH, 1p/19q codeletion, and chromosome 7 gain and 10 loss were described. Upper bar graph indicates the number of alterations of each case. Right bar graph indicates the number of cases exhibiting alterations of each gene. Figure S2. Extensive infiltration of the deep white matter observed in histopathological findings. T2-weighted images of initial tumor and terminal stage (left). Macroscopic images of each site obtained during autopsy (middle). Hematoxylin-eosin staining of the specimens from each site (right). Scale bar indicates 100 μ m. Figure S3. A Kaplan–Meier survival curve demonstrating progression-free survival (PFS) of the two groups based on white matter lesion (WML) scores (WML \leq 1 vs. WML $>$ 1). B Kaplan–Meier survival curve demonstrating overall survival (OS) of these two groups.

Additional file 2.

Acknowledgements

Not applicable.

Author contributions

Conception and design: YK, LC, FO, and RS; methodology development: YK, LC, and FO; data acquisition: YK, LC, FO, KM, NN, KA, SD, YS, JY, HS, SM, YT, RY, YO, AS, KK, and RS; data analysis and interpretation: YK, LC, and FO; manuscript writing: YK, LC, and FO.

Funding

This research was supported by Takeda Science Foundation.

Availability of data and materials

The datasets generated in this study will be made available upon reasonable request from the corresponding author.

Declarations

Ethics approval and consent to participate

This study was approved by the Institutional Review Board of Nagoya University Hospital (approval number: 2021-0451) and complied with all provisions of the World Medical Association Declaration of Helsinki. Tumor samples were collected intraoperatively after obtaining informed consent from the patients.

Consent for publication

Not applicable.

Competing interests

The authors declare that they have no competing interests.

Author details

¹Department of Neurosurgery, Nagoya University Graduate School of Medicine, 65 Tsurumai-cho, Showa-ku, Nagoya 466-8550, Japan. ²Division of Neurosurgery, Shizuoka Cancer Center, Nagaizumi, Japan. ³Division of Neurosurgery, Nagoya Central Hospital, Nagoya, Japan. ⁴Department of Virology, Nagoya City University Graduate School of Medical Sciences, Nagoya, Japan. ⁵Department of Pathology, Nagoya University Graduate School of Medicine, Nagoya, Japan. ⁶Department of Pathology and Laboratory Medicine, Graduate School of Medicine, Nagoya University, Nagoya, Japan.

Received: 22 August 2024 Accepted: 2 February 2025
Published online: 27 February 2025

References

- Anami S, Fukai J, Hama M, Awaya A, Inagaki T, Chiba T, Noda Y, Kanemura Y, Nakao N, Sonomura T (2021) Brainstem infiltration predicts survival in patients with high-grade gliomas treated with chemoradiotherapy. *Anticancer Res* 41:2583–2589. <https://doi.org/10.21873/anticancer.15037>
- Bette S, Gempt J, Huber T, Delbridge C, Meyer B, Zimmer C, Kirschke JS, Boeckh-Behrens T (2017) FLAIR signal increase of the fluid within the resection cavity after glioma surgery: Generally valid as early recurrence marker? *J Neurosurg* 127:417–425. <https://doi.org/10.3171/2016.8.Jns16752>
- Brown TJ, Brennan MC, Li M, Church EW, Brandmeir NJ, Rakszawski KL, Patel AS, Rizk EB, Suki D, Sawaya R et al (2016) Association of the extent of resection with survival in glioblastoma: a systematic review and meta-analysis. *JAMA Oncol* 2:1460–1469. <https://doi.org/10.1001/jamaoncol.2016.1373>
- Catani M, Thiebaut de Schotten M (2008) A diffusion tensor imaging tractography atlas for virtual in vivo dissections. *Cortex* 44:1105–1132. <https://doi.org/10.1016/j.cortex.2008.05.004>
- Chenevert TL, Malyarenko DI, Galbán CJ, Gomez-Hassan DM, Sundgren PC, Tsien CI, Ross BD (2019) Comparison of voxel-wise and histogram analyses of glioma ADC maps for prediction of early therapeutic change. *Tomography* 5:7–14. <https://doi.org/10.18383/j.tom.2018.00049>
- Cheng Y, Bao W, Wu Q (2020) Cerebral hemispheric glioblastoma with PNET-like morphology and histone H3.3 G34 mutation in younger patients: report of three rare cases and diagnostic pitfalls. *Indian J Pathol Microbiol* 63:262–266. https://doi.org/10.4103/ijpm.ijpm_544_19
- Crowell C, Mata-Mbemba D, Bennett J, Matheson K, Mackley M, Perreault S, Erker C (2022) Systematic review of diffuse hemispheric glioma, H3 G34-mutant: outcomes and associated clinical factors. *Neurooncol Adv* 4:vdac133. <https://doi.org/10.1093/oaajnl/vdac133>
- Drumm MR, Dixit KS, Grimm S, Kumthekar P, Lukas RV, Raizer JJ, Stupp R, Chheda MG, Kam KL, McCord M et al (2020) Extensive brainstem infiltration, not mass effect, is a common feature of end-stage cerebral glioblastomas. *Neuro Oncol* 22:470–479. <https://doi.org/10.1093/neuonc/noz216>
- Duffau H (2024) Damaging a few millimeters of the deep white matter tracts during glioma surgery may result in a large-scale brain disconnection. *J Neurosurg* 140:311–314. <https://doi.org/10.3171/2023.6.JNS231048>
- Fontebasso AM, Liu XY, Sturm D, Jabado N (2013) Chromatin remodeling defects in pediatric and young adult glioblastoma: a tale of a variant histone 3 tail. *Brain Pathol* 23:210–216. <https://doi.org/10.1111/bpa.12023>
- Gately L, McLachlan SA, Philip J, Ruben J, Dowling A (2018) Long-term survivors of glioblastoma: a closer look. *J Neurooncol* 136:155–162. <https://doi.org/10.1007/s11060-017-2635-1>
- Gessi M, Gielen GH, Hammes J, Dörner E, Az M, Waha A, Pietsch T (2013) H3.3 G34R mutations in pediatric primitive neuroectodermal tumors of central nervous system (CNS-PNET) and pediatric glioblastomas: Possible diagnostic and therapeutic implications? *J Neurooncol* 112:67–72. <https://doi.org/10.1007/s11060-012-1040-z>
- Grabowski MM, Recinos PF, Nowacki AS, Schroeder JL, Angelov L, Barnett GH, Vogelbaum MA (2014) Residual tumor volume versus extent of resection: predictors of survival after surgery for glioblastoma. *J Neurosurg* 121:1115–1123. <https://doi.org/10.3171/2014.7.Jns132449>
- Khuong-Quang DA, Buczkowicz P, Rakopoulos P, Liu XY, Fontebasso AM, Bouffet E, Bartels U, Albrecht S, Schwartzentruber J, Letourneau L et al (2012) K27M mutation in histone H3.3 defines clinically and biologically distinct subgroups of pediatric diffuse intrinsic pontine gliomas. *Acta Neuropathol* 124:439–447. <https://doi.org/10.1007/s00401-012-0998-0>
- Korshunov A, Capper D, Reuss D, Schrimpf D, Ryzhova M, Hovestadt V, Sturm D, Meyer J, Jones C, Zheludkova O et al (2016) Histologically distinct neuroepithelial tumors with histone 3 G34 mutation are molecularly similar and comprise a single nosologic entity. *Acta Neuropathol* 131:137–146. <https://doi.org/10.1007/s00401-015-1493-1>
- Kurokawa R, Baba A, Kurokawa M, Pinarbasi ES, Makise N, Ota Y, Kim J, Srinivasan A, Moritani T (2022) Neuroimaging features of diffuse hemispheric glioma, H3 G34-mutant: a case series and systematic review. *J Neuroimaging* 32:17–27. <https://doi.org/10.1111/jon.12939>
- Latini F, Fahlström M, Hesselager G, Zetterling M, Ryttefors M (2020) Differences in the preferential location and invasiveness of diffuse low-grade gliomas and their impact on outcome. *Cancer Med* 9:5446–5458. <https://doi.org/10.1002/cam4.3216>
- Laukamp KR, Lindemann F, Weckesser M, Hesselmann V, Ligges S, Wölfer J, Jeibmann A, Zinnhardt B, Viel T, Schäfers M et al (2017) Multimodal imaging of patients with gliomas confirms (11)C-MET PET as a complementary marker to MRI for noninvasive tumor grading and intraindividual follow-up after therapy. *Mol Imaging* 16:1536012116687651. <https://doi.org/10.1177/1536012116687651>
- Loit M, Rheault F, Gayat E (2019) Hotspots of small strokes in glioma surgery: An overlooked risk? *Acta Neurochir (Wien)* 161:91–98
- Louis DN, Perry A, Wesseling P, Brat DJ, Cree IA, Figarella-Branger D, Hawkins C, Ng HK, Pfister SM, Reifenberger G et al (2021) The 2021 WHO classification of tumors of the central nervous system: a summary. *Neuro Oncol* 23:1231–1251. <https://doi.org/10.1093/neuonc/noab106>
- Mackay A, Burford A, Carvalho D, Izquierdo E, Fazal-Salom J, Taylor KR, Bjerke L, Clarke M, Vinci M, Nandhabalan M et al (2017) Integrated molecular meta-analysis of 1,000 pediatric high-grade and diffuse intrinsic pontine glioma. *Cancer Cell* 32:520–537.e525. <https://doi.org/10.1016/j.ccell.2017.08.017>
- Molinaro AM, Hervey-Jumper S, Morshed RA, Young J, Han SJ, Chunduru P, Zhang Y, Phillips JJ, Shai A, Lafontaine M et al (2020) Association of maximal extent of resection of contrast-enhanced and non-contrast-enhanced tumor with survival within molecular subgroups of patients with newly diagnosed glioblastoma. *JAMA Oncol* 6:495–503. <https://doi.org/10.1001/jamaoncol.2019.6143>
- Mori R, Takeshima Y, Kawano T, Kuroda J-i, Takezaki T, Hayashi K, Shinjima N, Mukasa A (2022) A case of diffuse hemispheric glioma, H3 G34-mutant with PNET-like glioblastoma pathology. *Jpn J Neurosurg* 31:531–537. <https://doi.org/10.7887/jcns.31.531>
- Motomura K, Chalise L, Ohka F, Aoki K, Tanahashi K, Hirano M, Nishikawa T, Wakabayashi T, Natsume A (2018) Supratotal resection of diffuse frontal lower grade gliomas with awake brain mapping, preserving motor, language, and neurocognitive functions. *World Neurosurg* 119:30–39. <https://doi.org/10.1016/j.wneu.2018.07.193>
- Motomura K, Chalise L, Ohka F, Aoki K, Tanahashi K, Hirano M, Nishikawa T, Yamaguchi J, Shimizu H, Wakabayashi T et al (2021) Impact of the extent of resection on the survival of patients with grade II and III gliomas using awake brain mapping. *J Neurooncol* 153:361–372. <https://doi.org/10.1007/s11060-021-03776-w>
- Motomura K, Natsume A, Iijima K, Kuramitsu S, Fujii M, Yamamoto T, Mae-sawa S, Sugiura J, Wakabayashi T (2017) Surgical benefits of combined awake craniotomy and intraoperative magnetic resonance imaging for gliomas associated with eloquent areas. *J Neurosurg* 127:790–797. <https://doi.org/10.3171/2016.9.Jns16152>
- Nariai T, Tanaka Y, Wakimoto H, Aoyagi M, Tamaki M, Ishiwata K, Senda M, Ishii K, Hirakawa K, Ohno K (2005) Usefulness of L-[methyl-11C] methionine-positron emission tomography as a biological monitoring tool in the treatment of glioma. *J Neurosurg* 103:498–507. <https://doi.org/10.3171/jns.2005.103.3.0498>
- Neumann JE, Dorostkar MM, Korshunov A, Mawrin C, Koch A, Giese A, Schüller U (2016) Distinct histomorphology in molecular subgroups of glioblastomas in young patients. *J Neuropathol Exp Neurol* 75:408–414. <https://doi.org/10.1093/jnen/nlw015>
- Okita Y, Kinoshita M, Goto T, Kagawa N, Kishima H, Shimosegawa E, Hatazawa J, Hashimoto N, Yoshimine T (2010) (11)C-methionine uptake correlates with tumor cell density rather than with microvessel density in glioma: a stereotactic image-histology comparison. *Neuroimage* 49:2977–2982. <https://doi.org/10.1016/j.neuroimage.2009.11.024>
- Okochi Y, Nishihashi T, Fujii M, Kato K, Okada Y, Ando Y, Maesawa S, Takebayashi S, Wakabayashi T, Naganawa S (2014) Clinical use of (11)C-methionine and (18)F-FDG-PET for germinoma in central nervous system. *Ann Nucl Med* 28:94–102. <https://doi.org/10.1007/s12149-013-0787-4>
- Ottenhausen M, Krieg SM, Meyer B, Ringel F (2015) Functional preoperative and intraoperative mapping and monitoring: increasing safety and efficacy in glioma surgery. *Neurosurg Focus* 38:E3. <https://doi.org/10.3171/2014.10.Focus14611>
- Pekmezci M, Morshed RA, Chunduru P, Pandian B, Young J, Villanueva-Meyer JE, Tihan T, Sloan EA, Aghi MK, Molinaro AM et al (2021) Detection of glioma infiltration at the tumor margin using quantitative stimulated Raman scattering histology. *Sci Rep* 11:12162. <https://doi.org/10.1038/s41598-021-91648-8>

33. Picart T, Barrिताult M, Poncet D, Berner LP, Izquierdo C, Tabouret E, Figarella-Branger D, Idbaih A, Bielle F, Bourg V et al (2021) Characteristics of diffuse hemispheric gliomas, H3 G34-mutant in adults. *Neurooncol Adv* 3:vdab061. <https://doi.org/10.1093/oaajnl/vdab061>
34. Pramanik PP, Parmar HA, Mammoser AG, Junck LR, Kim MM, Tsien CI, Lawrence TS, Cao Y (2015) Hypercellularity components of glioblastoma identified by high b-value diffusion-weighted imaging. *Int J Radiat Oncol Biol Phys* 92:811–819. <https://doi.org/10.1016/j.ijrobp.2015.02.058>
35. Puntinet J, Dangouloff-Ros V, Saffroy R, Pagès M, Andreiulo F, Grill J, Puget S, Boddaert N, Varlet P (2018) Historadiological correlations in high-grade glioma with the histone 3.3 G34R mutation. *J Neuroradiol* 45:316–322. <https://doi.org/10.1016/j.neurad.2018.02.006>
36. Roh TH, Kang SG, Moon JH, Sung KS, Park HH, Kim SH, Kim EH, Hong CK, Suh CO, Chang JH (2019) Survival benefit of lobectomy over gross-total resection without lobectomy in cases of glioblastoma in the noneloquent area: a retrospective study. *J Neurosurg* 132:895–901. <https://doi.org/10.3171/2018.12.Jns182558>
37. Roux A, Pallud J, Saffroy R, Edjlali-Goujon M, Debily MA, Boddaert N, Sanson M, Puget S, Knafo S, Adam C et al (2020) High-grade gliomas in adolescents and young adults highlight histomolecular differences from their adult and pediatric counterparts. *Neuro Oncol* 22:1190–1202. <https://doi.org/10.1093/neuonc/noaa024>
38. Sanai N, Berger MS (2018) Surgical oncology for gliomas: the state of the art. *Nat Rev Clin Oncol* 15:112–125. <https://doi.org/10.1038/nrclinonc.2017.171>
39. Sanai N, Polley MY, McDermott MW, Parsa AT, Berger MS (2011) An extent of resection threshold for newly diagnosed glioblastomas. *J Neurosurg* 115:3–8. <https://doi.org/10.3171/2011.2.jns10998>
40. Schmahmann JD, Smith EE, Eichler FS, Filley CM (2008) Cerebral white matter: neuroanatomy, clinical neurology, and neurobehavioral correlates. *Ann NY Acad Sci* 1142:266–309. <https://doi.org/10.1196/annals.1444.017>
41. Smith JS, Chang EF, Lamborn KR, Chang SM, Prados MD, Cha S, Tihan T, Vandenberg S, McDermott MW, Berger MS (2008) Role of extent of resection in the long-term outcome of low-grade hemispheric gliomas. *J Clin Oncol* 26:1338–1345. <https://doi.org/10.1200/jco.2007.13.9337>
42. Sturm D, Bender S, Jones DT, Lichter P, Grill J, Becher O, Hawkins C, Majewski J, Jones C, Costello JF et al (2014) Paediatric and adult glioblastoma: multifactorial (epi)genomic culprits emerge. *Nat Rev Cancer* 14:92–107. <https://doi.org/10.1038/nrc3655>
43. Takeda M, Takahama T, Sakai K, Shimizu S, Watanabe S, Kawakami H, Tanaka K, Sato C, Hayashi H, Nonagase Y et al (2021) Clinical application of the FoundationOne CDx assay to therapeutic decision-making for patients with advanced solid tumors. *Oncologist* 26:e588–e596. <https://doi.org/10.1002/onco.13639>
44. Vettermann FJ, Felsberg J, Reifenberger G, Hasselblatt M, Forbrig R, Berding G, la Fougère C, Galldiks N, Schittenhelm J, Weis J et al (2018) Characterization of diffuse gliomas with histone H3-G34 mutation by MRI and dynamic 18F-FET PET. *Clin Nucl Med* 43:895–898. <https://doi.org/10.1097/rlu.0000000000002300>
45. Vuong HG, Le HT, Dunn IF (2022) The prognostic significance of further genotyping H3G34 diffuse hemispheric gliomas. *Cancer* 128:1907–1912. <https://doi.org/10.1002/cncr.34156>
46. Wu G, Broniscer A, McEachron TA, Lu C, Paugh BS, Becksfors J, Qu C, Ding L, Huether R, Parker M et al (2012) Somatic histone H3 alterations in pediatric diffuse intrinsic pontine gliomas and non-brainstem glioblastomas. *Nat Genet* 44:251–253. <https://doi.org/10.1038/ng.1102>
47. Yamada CAF, Soldatelli MD, de Amaral LLF, Campos CMS, de Moraes PL, Chaddad-Neto FEA, Lancellotti CLP (2023) Case report: evolutionary clinical-radiological features of a diffuse hemispheric glioma, H3 G34 mutant with over 5 years of survival. *Case Rep Oncol* 16:279–286. <https://doi.org/10.1159/000530181>
48. Yamaguchi J, Motomura K, Ohka F, Aoki K, Tanahashi K, Hirano M, Chalise L, Nishikawa T, Shimizu H, Natsume A et al (2021) Survival benefit of supratotal resection in a long-term survivor of IDH-wildtype glioblastoma: a case report and literature review. *NMC Case Rep J* 8:747–753. <https://doi.org/10.2176/nmccrj.cr.2021-0120>
49. Yoshimoto K, Hatae R, Sangatsuda Y, Suzuki SO, Hata N, Akagi Y, Kuga D, Hideki M, Yamashita K, Togao O et al (2017) Prevalence and clinicopathological features of H3.3 G34-mutant high-grade gliomas: a retrospective study of 411 consecutive glioma cases in a single institution. *Brain Tumor Pathol* 34:103–112. <https://doi.org/10.1007/s10014-017-0287-7>

Publisher's Note

Springer Nature remains neutral with regard to jurisdictional claims in published maps and institutional affiliations.